archives
of thermodynamics
Vol. **39**(2018), No. 4, 141–156
DOI: 10.1515/aoter-2018-0034

Numerical study of an air plane solar collector with the baffle in zigzag form

NABILA GUENDOUZ*
NACEREDDINE BIBI-TRIKI
FAOUZI DIDI
CHHAFIKA ZIDANI

Unit of Research on Materials and Renewable Energies, Department of Physics, Faculty of Sciences, Abou Bekr Belkaïd University, BP 119-13000-Tlemcen, Algerie

Abstract The production of thermal energy from solar energy by flat collectors finds nowadays many applications due to their innumerable economic and environmental interests. Currently, conservation of energy resources has become a global priority. On the other hand, given the dizzying demand for energy, has led specialists to find new techniques, such as renewable energies (solar, wind and geothermal). The present work is a contribution, by numerical simulation, to the study of heat transfer in flat solar collectors. On the basis of some experimental data, several simulation calculations have been carried out in order to determine the influencing parameters allowing better performance of the sensors and ensuring a good homogeneity of the temperature distributions. Based on the observation that, due to the low thermophysical properties of the air used as heat transfer fluid, solar air collectors rather give poor yields. It has been found very useful to have 'baffling' obstacles of various shapes and forms in the solar collector duct. This increases the thermal transfer of a coolant, which clearly improves the thermal efficiency of the solar air collector. This article consists mainly of studying the effects on heat transfer of turbulent forced convection by baffles of zigzag shapes, placed in a rectangular channel, using the finite volume method. The pressure-velocity coupling has been processed by the SIMPLEC algorithm. The results are presented in terms of the average Nusselt number and temperature field for different positions.

Keywords: Turbulent flow; Forced convection; Rectangular pipe; Baffle; Heat transfer

*Corresponding Author. Email: guendouznabila88@gmail.com

Nomenclature

C_f	–	friction coefficient
C_{f0}	–	friction coefficient without baffles
D	–	distance between two baffles, m
D_h	–	hydraulic diameter of channel, m
D_ω	–	crossing diffusion term, m/s
e	–	fin height, m
G_k	–	production of turbulent kinetic energy due to speed gradient, m/s
G_ω	–	production of kinetic energy due to buoyancy, m/s
h	–	baffle height, m
H	–	canal height, m
k	–	turbulent kinetic energy, m/s
L	–	channel length, m
L_1	–	distance upstream of the first baffle, m
L_2	–	distance downstream of the second baffle, m
L_3	–	distance length between the outlet and the second fin, m
P	–	pressure, Pa
Re	–	Reynolds number
P	–	pressure, Pa
Pr	–	Prandtl number
Nu	–	Nusselt number
T	–	temperature, K
T_b	–	bulk temperature (the temperature of the fluid that is 'far' from the wall), K
T_{in}	–	inlet temperature, K
T_W	–	temperature of the lower and upper walls, K
C_{pf}	–	specific heat of fluid, J/kg K
C_{ps}	–	specific heat of solid, J/kg K
S_k, S_ω	–	source term for k and ω
u_i	–	components of velocity in direction x_i, m/s
u_j	–	components of velocity in direction x_j, m/s
U_{in}	–	inlet velocity, m/s
U_{max}, V_{max}	–	maximum velocity
$\overline{U}$	–	average speed inside the channel, m/s
u, v	–	velocity of fluid in directions y, x, m/s
$\overline{v}$	–	velocity vector, m/s
x, x_i , x_j , y	–	Cartesian coordinates, m
Y_k, Y_x	–	dissipation of k and ω, m/s
$\overline{U}$	–	average speed through the section

Greek symbols

ΔP	–	pressure losses
δ	–	fin width, m
ε	–	turbulent dissipation energy, m^2/s^2

λ	–	thermal conductivity, W/m K
μ_e	–	effective viscosity, Pa s
μ_f	–	dynamic viscosity of fluid, kg/m s
ρ	–	air density, kg/m
ρ_f	–	density of air, kg/m^3
ρ_s	–	density of solid, kg/m^3
$\sigma_k,\ \sigma_g,\ \sigma_t\ \sigma_\omega$	–	constant value for the standard turbulence model of k-ω
τ_w	–	shear stress at the wall
Ψ	–	steam function
ω	–	dissipation rate of specific turbulence energy, m/s

Subscripts

in	–	inlet of the channel section
out	–	outlet of the channel section
t	–	turbulent
w	–	walls
f	–	fluid
s	–	solid

1 Introduction

Due to the insufficiency of heat exchange carried out in the plane air solar collector between the fluid and the absorber, it is interesting to make improvements for their better performance or better thermal efficiency. Ahmet *et al.* [1] examined the effect of the geometric parameters on the steady turbulent flow passing through a pipe with baffles. The effect of the orientation and the distance between nine baffles on the improvement of heat transfer was highlighted in this paper. Another experimental investigation was carried out by Molki *et al.* [2] to evaluate heat transfer and pressure losses in a rectangular channel with baffles.

Choudhury and Garg [3] used air-heating collectors with packed air flow channels, the purpose being to create turbulence and so to increase the heat transfer. Their theoretical study concluded that the use of obstacles (bed of grain of given specific conductivity) was beneficial for heat transfer. However, the increase in the pressure drop, especially beyond 2 m in length of collector requires a detailed optimization of the forms of grains.

Parkpoom *et al.* [4] investigated the influence of Z shaped baffle turbulators on heat transfer augmentation in a rectangular channel. They found that the, friction factor, Nusselt number and thermal performance characteristics for the in-phase 45° Z-baffle are considerably higher than those for the out-phase 45° Z-baffle at same operating condition. The in-phase 45° Z-baffle with larger e/H ratio provides higher heat transfer and friction

loss than the one with smaller e/H while the shorter pitch length yields the higher Nusselt numbar and , and thermodynamic enhancement factor (TEF) than the larger one.

Kellar and Patankar [5] presented the fluid flow and heat transfer in two-dimensional finned passages analyzed for constant property laminar flow. The passage is formed by two parallel plates to which fins are attached in a staggered fashion. Both the plates are maintained at a constant temperature. Streamwise periodic variation of the cross-sectional area causes the flow and temperature fields to repeat periodically after a certain developing length. Computations were performed for different values of the Reynolds number, Prandtl number, geometric parameters, and the fin-conductance parameter. The fins were found to cause the flow to deflect significantly and impinge upon the opposite wall so as to increase the heat transfer significantly. However, the associated increase in pressure drop was an order of magnitude higher than the increase in heat transfer. Streamline patterns and local heat transfer results are presented in addition to the overall results.

In the paper presented is experimental analysis of a single pass solar air collector with, and without baffle fin. The heat transfer coefficient between the absorber plate and air can be considerably increased by using artificial roughness on the bottom plate and under the absorber plate of a solar air heater duct. An experimental study has been conducted to investigate the effect of roughness and operating parameters on heat transfer. The investigation has covered the range of Reynolds number from 1259 to 2517, depending on types of the configuration of solar collectors. Based on the experimental data, values of Nusselt number Nu have been determined for different values of configurations and operating parameters. To determine the enhancement in heat transfer and increment in thermal efficiency, the values of Nusselt have been compared with those of smooth duct under similar flow conditions [6].

Menasrie and Moumi [7] established an empirical model for calculation of the coefficient of thermal exchange by convection, during the air flow in a rectangular duct, whose lower plan is equipped with baffles of rectangular forms laid out in quincunx. By the method of the dimensional analysis, they were able to relate all the physical, thermophysical parameters, and the geometrical characteristics of the baffles, and according to the mode of flow estimated a coefficient of exchange by convection.

Rajendra *et al.* [8] conducted an experimental work on the study of

heat transfer and friction in rectangular ducts with baffles (solid or perforated) attached to one of the broad walls. The Reynolds number of the study ranges from 2850 to 11500. The baffled wall of the duct is uniformly heated while the remaining three walls are insulated. These boundary conditions corresponded closely to those found in solar air heaters. Over the range of the study, the Nusselt number for the solid baffles is higher than that for the smooth duct, as well as for the perforated baffles. The friction factor for the solid baffles is found to be 9.6–11.1 times of the smooth duct, which decreased significantly for the perforated baffles with the increase in the open area ratio. Performance comparison with the smooth duct at equal pumping power shows that the baffles with the highest open area ratio give the best performance.

An experimental study was conducted by Molki and Mostoufizadeh [9] to investigate heat transfer and pressure drop in a rectangular duct with repeated-baffle blockages. The baffles are arranged in a staggered fashion with fixed axial spacing. The transfer coefficients are evaluated in the periodic fully developed and entrance regions of the duct. The presence of the baffles enhances these coefficients. The entrance length of the duct is substantially reduced by the baffles. Pressure drop and heat transfer data are employed to evaluate the thermal performance of the duct.

2 Mathematical formulation

2.1 Geometry of the problem

The geometry of the problem is presented in Fig. 1. It is a rectangular duct, equipped with two zigzag-shaped baffles, traversed by a stationary turbulent air flow which satisfies the following hypotheses:

- physical properties of air are assumed to be constant.
- velocity profile is uniform at the channel entrance.
- flow is considered as steady.
- effects of induced buoyancy are supposed to be negligible.
- thermophysical properties of the fluid $(C_{pf}, \mu, \lambda_f, \rho_f)$ and of solid $(C_{ps}, \lambda_s, \rho_s)$ are constant and evaluated at the temperature of the fluid at the entrance of the channel uniform temperature profile at the channel inlet.

- temperatures of the upper and lower walls are constant. Based on the experimental work of Demartini *et al.* [12], it was decided to carry out an air flow test under the following conditions: channel length $L = 0.554$ m, channel height $H = 0.143$ m, fin height $e = 0.08$ m, distance between the canal inlet and the first wing $L_1 = 0.223$ m, spacing between the two wings $L_2 = 0.152$ m, distance between the second wing and the channel outlet $L_3 = 0.179$ m, hydraulic diameter $D_h = 0.14$ m, Reynolds number Re $= 5000$, input velocity $U_{in} = 0.45$ m/s.

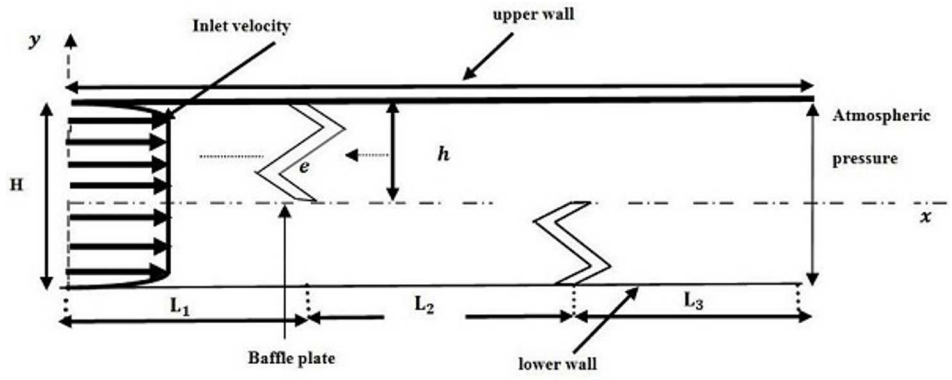

Figure 1: Representative diagram of the problem.

2.2 Governing equations

The flow equations (i.e., continuity, momentum) used to simulate the incompressible and steady flow of air in the given area of computation are given by:

- Conservation of mass:

$$\frac{\partial(\rho u)}{\partial x} + \frac{\partial(\rho v)}{\partial y} = 0 \,. \tag{1}$$

- Conservation of momentum:

$$\rho u\frac{\partial u}{\partial x} + \rho v\frac{\partial u}{\partial y} = -\frac{\partial P}{\partial X} + \frac{\partial}{\partial x}\left[(\mu+\mu_t)\left(2\frac{\partial u}{\partial x}\right)\right] \frac{\partial}{\partial y}\left[(\mu+\mu_t)\left(\frac{\partial u}{\partial y} + \frac{\partial v}{\partial x}\right)\right] , \tag{2}$$

$$\rho u\frac{\partial v}{\partial x}+\rho v\frac{\partial T}{\partial y}=-\frac{\partial P}{\partial X}+\frac{\partial}{\partial x}\left[(\mu+\mu_t)\left(2\frac{\partial v}{\partial x}\right)\right]\frac{\partial}{\partial y}\left[(\mu+\mu_t)\left(\frac{\partial u}{\partial y}+\frac{\partial v}{\partial x}\right)\right]. \tag{3}$$

- Conservation of energy inside the fluid:

$$\rho u\frac{\partial T}{\partial x}+\rho v\frac{\partial T}{\partial y}=\frac{\partial}{\partial x}\left[\left(\frac{\mu}{\mathrm{Pr}}+\frac{\mu_t}{\sigma_T}\right)\frac{\partial T}{\partial x}\right]+\frac{\partial}{\partial y}\left[\left(\frac{\mu}{\mathrm{Pr}}+\frac{\mu_t}{\sigma_T}\right)\frac{\partial T}{\partial y}\right]. \tag{4}$$

- Conservation of energy in the wall:

$$\left(\frac{\partial^2 T}{\partial x^2}+\frac{\partial^2 T}{\partial y^2}\right)=0\,. \tag{5}$$

2.3 Equations of turbulence

A comparative study was conducted on four models of turbulence, namely the Spalart Allamaras model, the (k-ε) model, the (k-ω) model and the Reynolds voltage model, which were evaluated through the resolution of the Navier-Stokes equations. It has been found that the (k-ε) model is the most accurate in predicting flow changes in the presence of baffles [10].

The chosen turbulence model allowed us to calculate the rapidly changing two-dimensional flux and also to anticipate the interactions with the wall. Another advantage of the selected turbulence model is that the model equations behave suitably in the regions both in the vicinity of the wall and far away from it as well. The (k-ω) model is defined by two transport equations, one for the turbulent kinetic energy k and the other for the specific dissipation rate ω [11]:

$$\frac{\partial}{\partial t}(\rho k)+\frac{\partial}{\partial x_i}(\rho k u_i)=\frac{\partial}{\partial x_j}\left(\Gamma_k\frac{\partial k}{\partial x_j}\right)+G_k-Y_k+S_k\,, \tag{6}$$

$$\frac{\partial}{\partial t}(\rho\omega)+\frac{\partial}{\partial x_i}(\rho\omega u_i)=\frac{\partial}{\partial x_j}\left(\Gamma_\omega\frac{\partial \omega}{\partial x_j}\right)+G_\omega-Y_\omega+D_\omega+S_\omega\,, \tag{7}$$

where

$$G_k=-\rho\overline{u_i' u_j'}\frac{\delta u_j}{\delta x_i},\quad G_\omega=\alpha\frac{\omega}{k}G_k\,, \tag{8}$$

$$\Gamma_k=\mu+\frac{\mu_t}{\sigma_k},\quad \Gamma_\omega=\mu+\frac{\mu_t}{\sigma_\omega}\,, \tag{9}$$

here the overbar denotes an average.

In general, the main sources of errors in the Nusselt numbers results

are the statistical uncertainty of the average surface temperature and fluid mass temperature. The calculation is locked in a cycle and the difference between wall temperature and bulk (average) temperature [5].

$$T_{f,m} = T_b(x) = \frac{\int_A u\,(x,y)\,T\,(x,y)\,dA}{\int_A u\,(x,y)\,dA}\,. \tag{10}$$

The resulting on average value of the Nusselt number are as follows:

$$\mathrm{Nu}\,(x) = \frac{h(x)D_h}{\lambda_f} = \frac{q_W D_h}{\lambda_f(T_W - T_b)} \tag{11}$$

and

$$\overline{\mathrm{Nu}} = \frac{\overline{h}D_h}{\lambda_f}\,. \tag{12}$$

2.4 Boundary conditions

(i) A uniform velocity was applied, as a boundary condition, and the pressure was set to zero at the entrance to the computational domain.

(ii) Two horizontal walls of the computational domain were both held at the constant temperature of 375 K. This constitutes a thermal boundary condition.

(iii) Temperature of the fluid used was set at 300 K at the inlet to the channel.

The finite volume method has been applied for the numerical resolution of the system of equations described above. The SIMPLEC algorithm proposed by Patankar [5] was used for pressure and velocity correction.

The Quick scheme is used for the discretization of the terms of convection and diffusion. A structured and non-uniform mesh was used, depending on the case under study, with a refined mesh in the areas containing the baffles and near the walls, in order to capture the strong gradients of temperature and velocity. Several tests were performed in order to ensure that the results do not depend on the refining of the mesh. The iterative procedure was continued until the residuals for all computing cells were less than 10^{-8} for all the quantities analyzed.

3 Results and interpretation

3.1 Mesh validation

Different grids were tested for the validity of the mesh and the accuracy of calculations. The results have been obtained for horizontal and vertical velocities U_{max} and V_{max}, respectively, and stream function Ψ.

Table 1: Comparison of results for different mesh grids.

Parameter	Unit	Mesh grid			
		40 × 10	50 × 15	60 × 20	70 × 25
Ψ_{max}	m^2/s	0.08577815	0.08771847	0.0881338	0.08923231
U_{max}	m/s	1.43087190	1.46323847	1.4701667	1.48849090
V_{max}	m/s	0.02343008	0.02396007	0.02407352	0.02437357

Parameter	Unit	Mesh grid			
		80 × 30	90 × 35	100 × 40	110 × 45
Ψ_{max}	m^2/s	0.09018343	0.09053433	0.09169389	0.092492267
U_{max}	m/s	1.50435660	1.51021013	1.52955272	1.53898930
V_{max}	m/s	0.02463337	0.02472922	0.0250459	0.02530724

For the Reynolds number equal to 5000, the results are presented in Tab. 1. For the remainder of the study, we chose the grid (100×40) which provides a precision fit and a relative error between the values found less than 1.25%.

3.2 Validation of the model

To validate our numerical modeling, the results obtained were compared with those reported in the work by Demartini *et al.* [13] who experimentally studied the dynamic behavior of air flow inside the rectangular duct equipped with plane baffles, with a Reynolds number equal to 5000. Comparing the results obtained for the axial velocity with the experimental ones due to Demartini *et al.* [12], as presented in Fig. 2, and for the axial position $x = 0$ m, one can note that the two series of results are in good agreement.

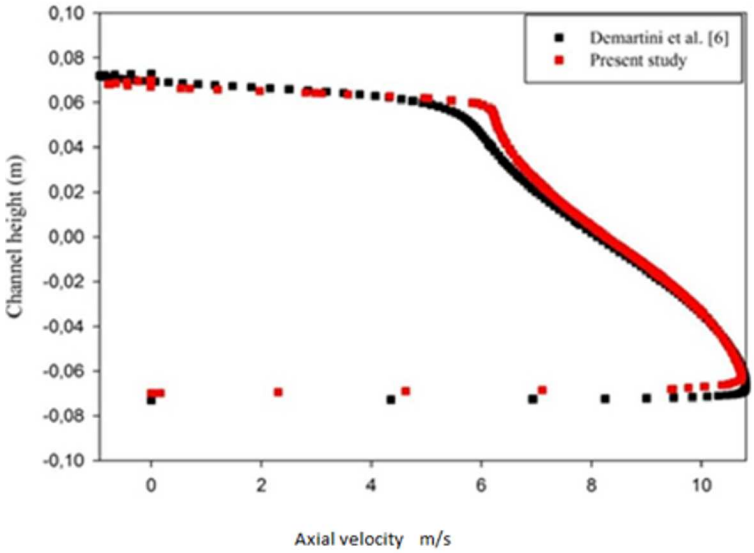

Figure 2: Validation of the numerical simulation with the experimental results of Dermatini *et al.* [12], for the position $x = 0.159$ m.

3.3 Hydrodynamic aspect

Figure 3 shows that the velocity values are very low in the vicinity of the two baffles, especially in the downstream regions, due to the presence of the recirculation zones. The highest speed values appear near the top of the channel, with an acceleration that begins just after the second baffle.

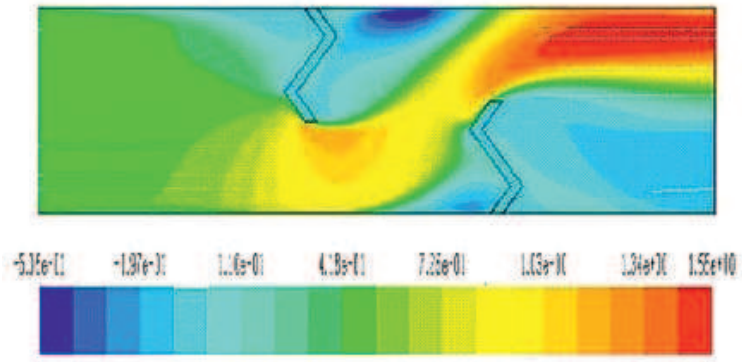

Figure 3: Contour of the axial velocity.

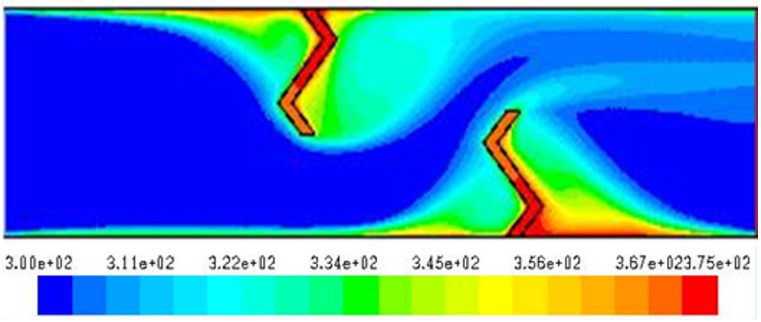

Figure 4: Contour of the temperature total.

Figure 4 shows that the temperature of air in the recirculation zones (after each fin) is substantially high. A drop in temperature in the areas upstream of each fin is observed. The areas with highest temperature are, for the most part, located in the vicinity of the walls and at the ends of the fins.

Five sections were chosen to carry out the hydrodynamic study. These are respectively: $x = 0.159$ m, 0.189 m, 0.225 m, 0.285 m, 0.315 m, 0.345 m, and 0.525 m, with respect to the channel inlet.

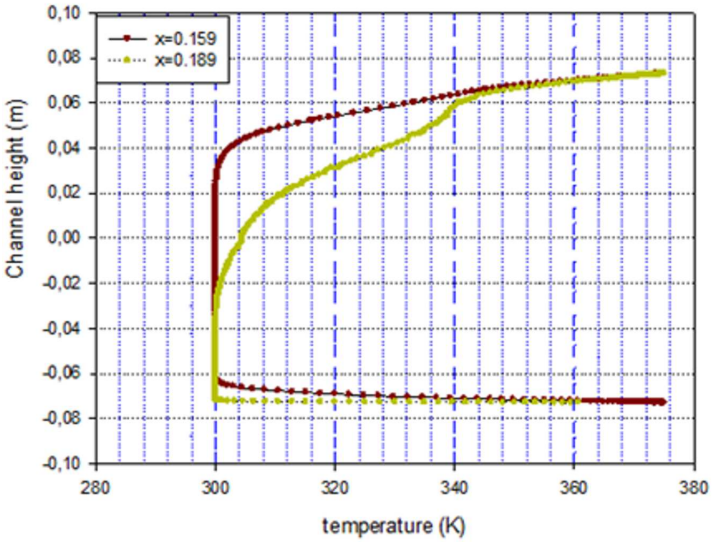

Figure 5: Temperature profile upstream of the first baffle.

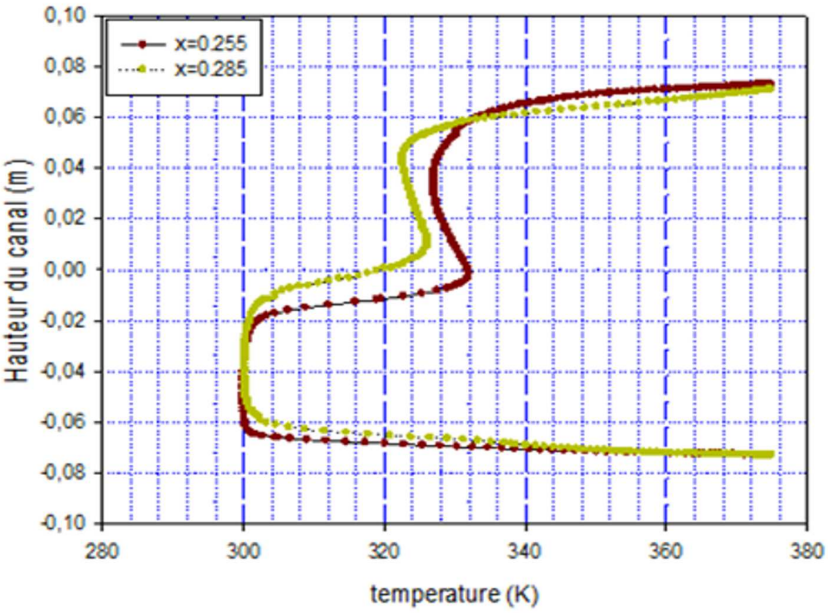

Figure 6: Temperature profile downstream of the first baffle.

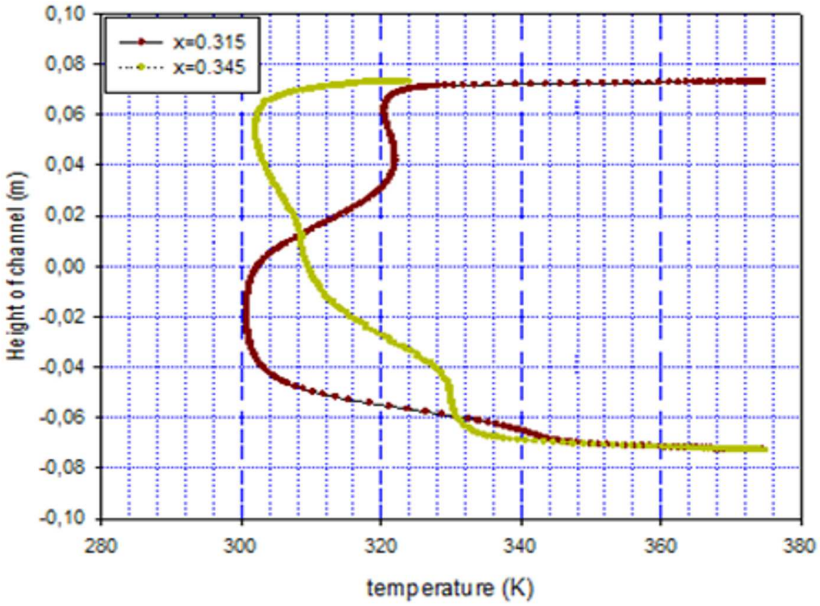

Figure 7: Temperature profiles upstream of the second baffle.

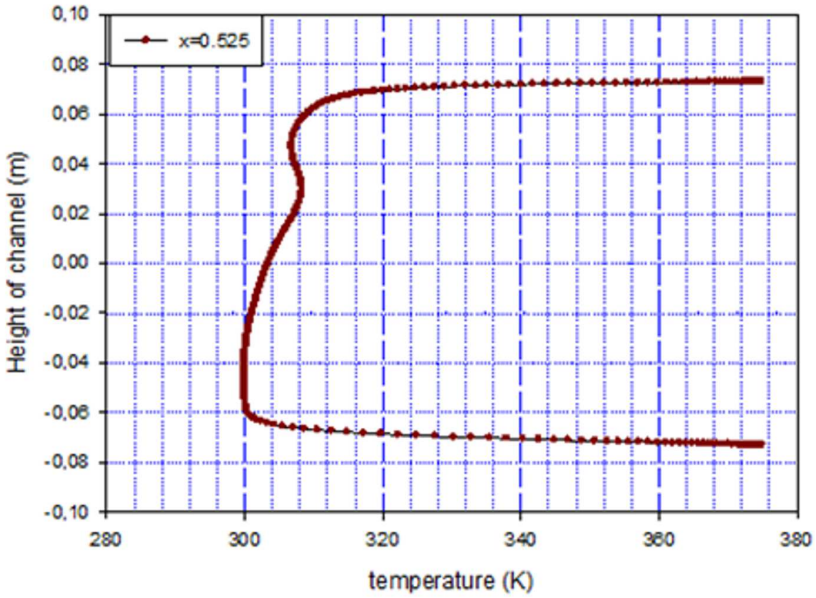

Figure 8: Temperature profile near the channel exit.

The numerical results represented by the temperature profiles for the sections $x = 0.159$ m, and 0.189 m, are shown in Figs. 5–8. These sections are located upstream of the first fin, located at $x = 0.223$ m from the entrance.

The presence of the first baffle located in the upper half of the channel induces a sharp increase in temperature. Between the two fins, at the locations $x = 0.225$ m and $x = 0.285$ m from the inlet, the flow is characterized by very high temperatures because the sections closest to the fins are always better heated as shown in Fig. 6. It is found that the flow approaching the second baffle, its temperature is increased in the lower part of the channel. At the outlet of the channel, for $x = 0.525$ m, the temperature profiles in Fig. 8 are presented. The values of the temperatures are decreasing since the exit of the channel is approached. The section is remote from the fins.

The growth of the Nusselt number towards its maximum value, found first in the central part, between the two fins and at the exit of the channel, is the result of intense acceleration of the recirculation of the flow in this zone that favors an increase in heat exchange Fig. 9.

The Nusselt number profile determined for different values of the Reynolds number: 5000, 10000, 15000, 20000, and 25000, Fig. 10. The number of Nusselt increases with the Reynolds number. These profiles present in

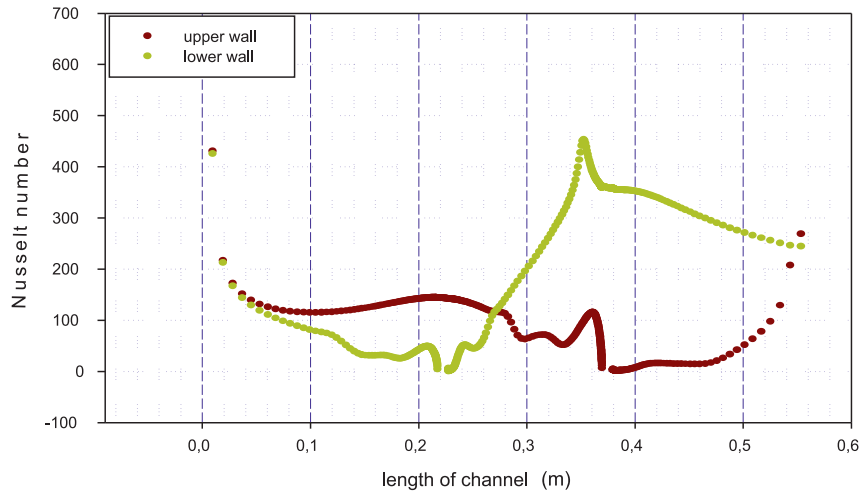

Figure 9: Variation of the Nusselt number on the lower and upper walls of the channel.

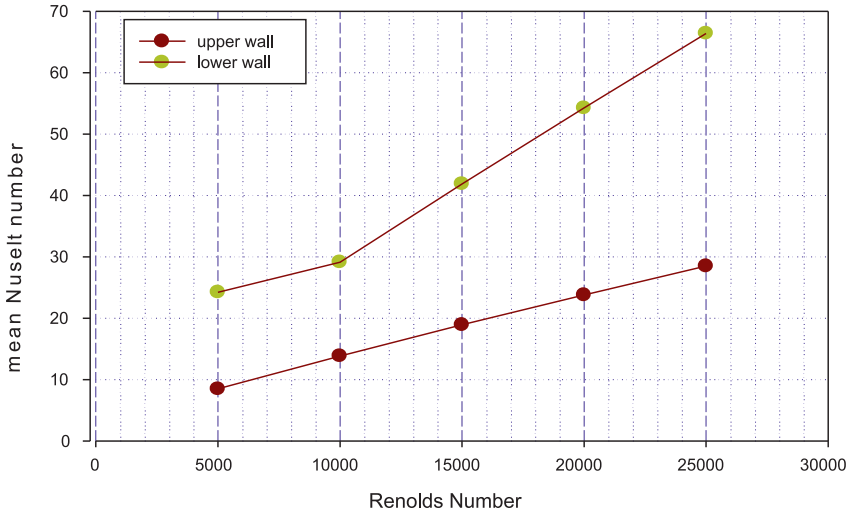

Figure 10: Variation of mean Nusselt number versus Reynolds number along the upper and lower wall of the channel.

all cases the minimum and the maximum of the Nusselt number. The minimum value, located in the first part of the channel, is due to the beginning of heating of air in the presence of the first fin which is in the upper half of the channel and which induces a strong decrease of the velocity. The Nusselt number increases with increasing Reynolds number of air. This is because the Nusselt number depends on the rate of heat transfer.

4 Conclusion

The analysis of the results obtained made it possible to associate increases in fluid temperature by the effect of baffles and fins at the outlet of each section. The numerical results obtained and presented allow to analyze the thermal behavior of a flow in a flat air solar collector with baffles. These results are an important contribution to the enrichment of knowledge on forced convection inside pipes.

The presence of the fins reduces the region of entry, it is in this part where the thermal exchanges are more important. The temperature of the air increases as soon as the fluid is again in contact with the baffles.

Finally, these swirling zones (recirculation) are responsible for local variations in the number of Nusselt along the surfaces of the baffles and the wall, particularly at the lower side of the wall. The highest heat transfer disturbances are obtained behind the second baffle and are caused by the formation of hot pockets in these areas.

All previous studies on the thermal or dynamic behavior of the different geometries of baffles does not ensure optimal models and hence of the advantages and disadvantages of each geometry used. So for future work, the best proposed baffle geometry will be the one that will ensure the highest heat transfer rate.

Received 27 May 2018

References

[1] Tandiroglu A.: *Effect of flow geometry parameters on transient heat transfer for turbulent flow in a circular tube with baffle insert*. Int. J. Heat. Mass Tran. **49**(2006), 9, 1559–1567.

[2] Molki M., Mostoufizadeh A.R.: *Turbulent Heat transfer in rectangular ducts with repeated-baffle blockages*. Int. J. Heat. Mass Tran. **32**(1989), 8, 1491–1499.

[3] Choudhury C., Garg H.P.: *Performance of air heating collectors with packed air flow passage*. Sol. Energy **505**(199), 205–221.

[4] Parkpoom Sriromreun, Chinaruk Thianpong, Pongjet Promvonge: *Experimental and numerical study on heat transfer enhancement in a channel with Zshaped baffles*. Int. Commun. Heat Mass **39**(2012), 7, 945–952.

[5] Kelkar K.M., Patankar S.V.: *Numerical prediction of flow and heat transfer in parallel plate channel with staggered fins*. J. Heat Transfer **109**(1987), 1, 25–30.

[6] Foued Chabane, Nesrine Hatraf: *Experimental study of heat transfer coefficient with rectangular baffle fin of solar air heater*. Front. Energ. **8**(2014), 2, 160–172.

[7] Menasria F., Moummi A.: *Modélisation des échanges convectifs dans le conduit utile dñun capteur solaire plan à air muni de rugosités artificielles de formes rectangulaires* . Rev. Energ. Renouv. **14**(2011), 3, 369–379.

[8] Rajendra K., Maheshwarib B.K., Karwac N.: *Experimental study of heat transfer enhancement in an asymmetrically heated rectangular duct with perforated baffles*. Int. Commun. Heat Mass **32**(2005), 1-2, 275–284.

[9] Molki M., Mostoufizadeh A.R.: *Turbulent heat transfer in rectangular ducts with repeated-baffle blockages*. Int. J. Heat Mass Transfer **32**(1989), 8, 1491–1499.

[10] Nasiruddin M.H., Kamran Siddiqui: *Heat transfer augmentation in a heat exchanger tube using a baffle*. Int. J. Heat Fluid Fl. **28**(2007), 2, 318–328.

[11] Ward S.: *Optimization of the forms and provisions of obstacles in the mobile air vein of solar air collectors at two air layers for the maximization of the couple efficiency-rise in temperature*. MSc thesis, University of Valenciennes, France, 1989.

[12] Dermatni L.C., Vielmo H.A., Moller S.V.: *Numeric and experimental analysis of the turbulent flow through a channel with baffle plates*. J. Braz. Soc. Mech. Sci. & Eng. **26**(2004), 2.